Structure and Properties of Poly(vinyl alcohol)/Na+ Montmorillonite Nanocomposites

K. E. Strawhecker and E. Manias*

Department of Materials Science and Engineering, The Pennsylvania State University, University Park, Pennsylvania 16802

Poly(vinyl alcohol)/sodium montmorillonite nanocomposites of various compositions were created by casting from a polymer/silicate water suspension. The composite structure study revealed a coexistence of exfoliated and intercalated MMT layers, especially for low and moderate silicate loadings. The inorganic layers promote a new crystalline phase different than the one of the respective neat PVA, characterized by higher melting temperature and a different crystal structure. This new crystal phase reflects on the composite materials properties. Namely, the hybrid polymer/silicate systems have mechanical, thermal, and water vapor transmission properties, which are superior to that of the neat polymer and its conventionally filled composites. For example, for a 5 wt % MMT exfoliated composite, the softening temperature increases by 25 °C and the Young's modulus triples with a decrease of only 20% in toughness, whereas there is also a 60% reduction in the water permeability. Furthermore, due to the nanoscale dispersion of filler, the nanocomposites retain their optical clarity.

Introduction

Polymer/layered-silicate hybrids—nanocomposites—have attracted strong interest in today's materials research, as it is possible to achieve impressive enhancements of material properties compared to the pure polymers. Especially when these properties depend on the surface area of the filler particles, small amounts (typically less than 5%) of nanometer-thin layered inorganic fillers give rise to the same level of mechanical and thermal improvements as are typically achieved with loadings of 30–50% of micron-sized fillers. Examples of such materials enhancements are decreased permeability to gases and liquids, better resistance to solvents, increased thermal stability, and improved mechanical properties. Nanometer-thin layered materials used to form polymer nanocomposites include montmorillonite clays, synthetic 2:1 aluminosilicates, metal phosphates, transition metal chalcogenides, and complex oxides, to name a few.[1-6] In some cases, properties are observed in nanoscale materials that have not been realized in more conventional material structures, as for example flame-retardant character.[7]

Sodium montmorillonite (MMT) is a naturally occurring 2:1 phyllosilicate, capable of forming stable suspensions in water. This hydrophilic character of MMT also promotes dispersion of these inorganic crystalline layers in water-soluble polymers such as poly(vinyl alcohol)[8] and poly(ethylene oxide)[9,10] Inspired from those studies, this work is focused on investigating the properties of poly(vinyl alcohol)/MMT nanocomposite hybrids. Poly(vinyl alcohol) (PVA) is a water-soluble polymer extensively used in paper coating, textile sizing, and flexible water-soluble packaging films.[11] These same applications stimulate an interest in improving mechanical, thermal, and permeability properties of thin nanocomposite films, ultimately with the hope of retaining the optical clarity of PVA. PVA/layered silicate nanocomposite materials may offer a viable alternative for these applications to heat treatments (that may cause polymer degradation) or conventionally filled PVA materials (that are optically opaque).

The present work explores first the structure of PVA/ MMT nanocomposite materials spanning the complete range of inorganic (MMT) loadings. Subsequently, we

* Address correspondence to manias@psu.edu.
(1) Giannelis, E. P.; Krishnamoorti, R. K.; Manias, E. *Adv. Polym. Sci.* **1998**, *138*, 107.
(2) Kojima, Y.; Usuki, A.; Kawasumi, M.; Okada, A.; Kurauchi, T. T.; Kamigaito, O. *J. Polym. Sci., Part A: Polym. Chem.* **1993**, *31*, 983. (b) Kojima, Y.; et al. *J. Polym. Sci., Part B: Polym. Phys.* **1995**, *33*, 1039.
(3) Lan, T.; Kaviratna, P. D.; Pinnavaia, T. J. *Chem. Mater.* **1995**, *7*, 2144. (b) Wang, M. S.; Pinnavaia, T. J. *Chem. Mater.* **1994**, *6*, 468. (c) Pinnavaia, T. J. *Science* **1983**, *220*, 365.
(4) Kanatzidis, M. G.; Wu, C. G.; Marcy, H. O.; DeGroot, D. C. Kannewurf, C. R. *Chem. Mater.* **1990**, *2*, 222. (b) *Chem. Mater.* **1991**, *3*, 992. (c) *Chem. Mater.* **1996**, *8*, 525.
(5) Vaia, R. A.; Ishii, H.; Giannelis, E. P. *Chem. Mater.* **1993**, *5*, 1694. (b) Vaia, R. A.; Jandt, K. D.; Kramer, E. J.; Giannelis, E. P. *Macromolecules* **1995**, *28*, 8080. (c) Vaia, R. A.; Price, G.; Ruth, P. N.; Nguyen, H. T.; Lichtenhan, J. *Appl. Clay Sci.* **1999**, *15*, 67.
(6) Krishnamoorti, R. K.; Vaia, R. A.; Giannelis, E. P. *Chem. Mater.* **1996**, *8*, 1728. (b) Giannelis, E. P. *Adv. Mater.* **1996**, *8*, 29.
(7) Gilman, J. W.; Jackson, C. L.; Morgan, A. B.; Harris, R.; Manias, E.; Giannelis, E. P.; Wuthenow, M.; Hilton, D.; Philips, S. H. *Chem. Mater.* **2000**, *12*, 1866.
(8) Carrado, K. A.; Thiyagarajan, P.; Elder, D. L. *Clays Clay Mineral.* **1996**, *44*, 506.
(9) Vaia, R. A.; Vasudevan, S.; Krawiec, W.; Scanlon, L. G.; Giannelis, E. P. *Adv. Mater.* **1995**, *7*, 154. (b) Vaia, R. A.; Sauer, B. B.; Tse, O. K.; Giannelis, E. P. *J. Polym. Sci., Part B: Polym. Phys.* **1997**, *35*, 59.
(10) Wong, S.; Vaia, R. A.; Giannelis, E. P.; Zax, D. B. *Solid State Ionics* **1996**, *86*, 547.
(11) Bassner S. L.; Klingenberg, E. H. *Am. Ceram. Soc. Bull.* **June 1998**, 71.

focus on a comparative study of the thermal, mechanical, and optical properties of pure PVA and PVA/MMT nanocomposites, with the emphasis on the application relevant, low silicate concentration (≤10 wt %) hybrid materials.
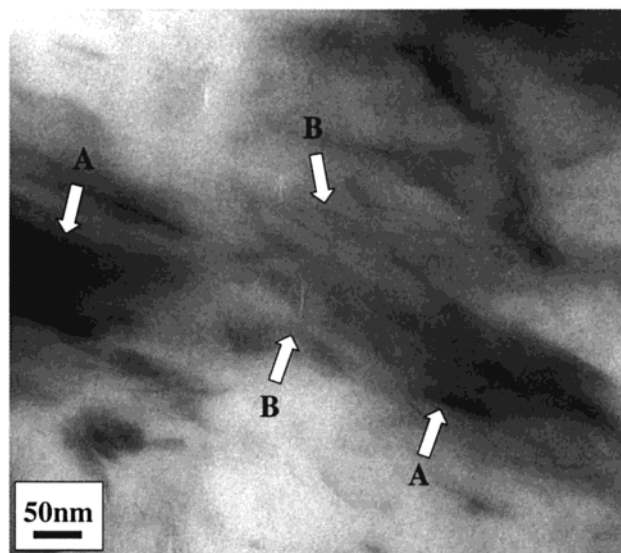
Experimental Section

Nanocomposite Formation. Nanocomposites were synthesized by a solution-intercalation film-casting method: hybrid films were cast from a MMT/water suspension where PVA was dissolved. Room temperature distilled water was used to form a suspension of sodium montmorillonite (Cloisite Na$^+$, Southern Clay Products, TX) at a concentration of ≤2.5 wt %. The suspension was stirred for 1 h and sonicated for 30 min. Low-viscosity, fully hydrolyzed (98.0−98.8%) atactic poly(vinyl alcohol) (Airvol 107, Air Products, PA) was added to the stirring suspensions such that the total solids (silicate plus polymer) concentration was ≤5 wt %. The mixtures were then heated to 90 °C to dissolve the PVA, again sonicated for 30 min, and finally films were cast in a closed oven at 40 °C for 2 days. We controlled the film thickness from 0.001 to 0.1 cm by varying the total starting solution volume. The polymer/MMT loading was defined by stoichiometric addition of polymer and silicate in the water suspension and was verified a posteriori by TGA.

Samples for water vapor transmission (WVT) and for UV/vis were prepared by cutting pieces of the cast films. The samples for the UV/vis measurements were further dried under vacuum at 80−90 °C for 24 h. The nanocomposites used for the other property and structure studies (TGA, XRD, TEM, and DSC) were films cast as described above; they were subsequently ground into powder and further dried under vacuum at 80−90 °C (PVA $T_g \simeq$ 70 °C) for at least 24 h. According to the TGA data, this results in less than 0.7% water content for pure PVA. For TEM studies, a piece of one film (80:20) was placed in epoxy resin and later microtomed into ca. 200 nm slices, which were placed upon nickel TEM grids.

Characterization. Wide-angle X-ray diffraction (XRD) data were collected in digital form using a Rigaku Geigerflex powder diffractometer with a Dmax-B controller and a vertical goniometer. Operation was in the $\theta-\theta$ geometry. The instrument uses radiation from a copper target tube (Cu Kα radiation λ = 1.541 871 Å, including both the Cu K$_\alpha^1$ and K$_\alpha^2$, whereas Cu K$_\beta$ was eliminated with a graphite monochromator). Transmission electron microscopy (TEM) was performed in a Hitachi HF-2000, which uses a high-vacuum cold-cathode field emission gun as the electron source, and bright field images were obtained. Differential scanning calorimetry (DSC) was performed in a Perkin-Elmer DSC7 at a heating (or cooling) rate of 20 °C/min under an argon atmosphere. Mechanical properties were investigated using an Instron tensile tester with sample films 22 mm in length and 5 mm in width, in an atmosphere of 50% relative humidity with a strain rate of 25 mm/min (as per ASTM D882-95a).[12] Water vapor transmission rates were studied following ASTM E96, "Standard Test Methods for Water Vapor Transmission of Materials".[13] Thermogravimetric analysis (TGA) was performed using a Perkin-Elmer TGA7 with a heating rate of 10 °C/min under an air atmosphere. UV/vis transmittance spectra were obtained using a Perkin-Elmer Lambda 2S UV/vis spectrometer at a wavelength scan rate of 60 nm/min.

Hybrid Structure and Materials Properties

The purpose of this study is, first, to investigate the structure of the PVA/MMT nanocomposites, with the

(12) ASTM standard, D 882-95a, Standard Test Method for Tensile Properties of Thin Plastic Sheeting, *Anual Book of ASTM Standards*, April 1995, p 182.

(13) ASTM standard, E 96-95, Standard Test Methods for Water Vapor Transmission of Materials, *Anual Book of ASTM Standards*, April 1999, p 829.

Figure 1. TEM image of 20 wt % MMT/PVA nanocomposite revealing the coexistence of intercalated (A) and exfoliated (B) MMT layers.

focus on the layered filler dispersion, as well as on the changes of the polymer crystallinity due to the inorganic layered fillers. Subsequently, through the study of selected nanocomposite material properties, we attempt to correlate the hybrid structure with changes in the material response. The structure is explored over the full range of silicate compositions. On the other hand, properties are explored only for the low silicate loadings, which are relevant to potential applications.

Dispersion of Inorganic Layers. Bright field TEM is used to directly view the hybrid structure for the nanocomposites formed, with the emphasis on the dispersion of the nanometer-thin layered fillers in the polymer matrix. A typical TEM image is shown in Figure 1 for the 20 wt % MMT nanocomposite. Extensive TEM observations reveal a coexistence of silicate layers in the intercalated (label "A") and the exfoliated ("B") states. We refer to intercalated layers/structures where the inorganic layers maintain the parallel registry of pristine silicates and are separated by ultrathin (1.3−5 nm) PVA films. Because of the periodic parallel assembly of the silicates, the intercalated structures give rise to X-ray diffraction peaks. We refer to exfoliated layers/structures where the layers are much further apart (≫5 nm), and in general both the layer registry and the parallel stacking are lost.

The periodic intercalated structure can be quantified through powder XRD. Comparison of the intercalated gallery height with that of the pristine MMT (9.7 Å) measures the thickness of the PVA/Na$^+$ film. Figure 2 shows XRD scans for concentrations of 20, 40, 60, 80, and 100 wt % MMT; the inset shows the corresponding d-spacing distributions for the same concentrations. The distribution of the intercalated d-spacings is calculated at half-maximum of the d_{001} peak, and the range of observed periodicities is given by bars (Figure 2, inset) for each sample. Both the d-spacings and their distributions decrease systematically with higher silicate loadings, from 40 to 90 wt % MMT. For lower inorganic filler concentrations, the XRD diffraction peak that corresponds to the silicate gallery d-spacing moves below 2θ = 1.5°. This suggests that, if there still exist periodic
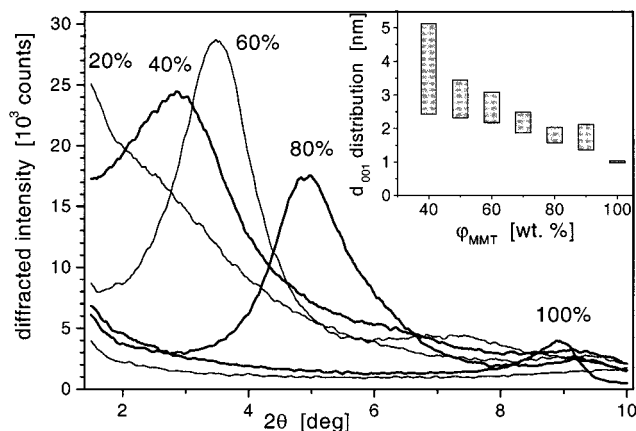
Figure 2. X-ray diffraction of the PVA/MMT hybrids as a function of ϕ_{MMT}. The inset shows the distribution of the MMT intercalated d-spacings for the respective hybrids.

assemblies of intercalated MMT layers, these are characterized by d-spacings larger than 5 nm. In addition, for all the nanocomposite XRDs, the background is higher than one would expect for simple mixtures of PVA and MMT, suggesting the existence of exfoliated inorganic layers throughout the polymer matrix. Thus, both XRD and TEM consistently show that these samples are in a hybrid structure where both intercalated and exfoliated silicate layers coexist in considerable ratios.

At first glance, this dependence of the intercalated structure and d-spacing on the polymer/silicate mass ratio seems to be at odds with the theoretical expectations.[14,15] The equilibrium hybrid structure predicted from the thermodynamics corresponds to an intercalated periodic nanocomposite (with a d-spacing around 1.8 nm) which is expected to be independent of the polymer/silicate composition.[14] However, thermodynamics can only predict the *equilibrium* structure. In our case, though, the hybrid structure that we find is actually kinetically dictated: In the water solution of poly(vinyl alcohol) and montmorillonite the layers remain in colloidal suspension. Where this suspension is slowly dried, the silicate layers remain distributed and embedded in the polymer gel. With further drying, to remove all water, although thermodynamics would predict the MMT layers to reaggregate in an intercalated fashion, the slow polymer dynamics trap some of the layers apart and therefore remain dispersed in the polymer. Obviously, these kinetic constraints by the polymer become less important as the polymer-to-silicate fraction decreases, and consequently, for higher ϕ_{MMT}, intercalated structures are formed. For these periodic structures, the variation of the d-spacing with ϕ_{MMT} reflects the different polymer/silicate weight ratios, and with increasing ϕ_{MMT} the intercalated d-spacing converges to the equilibrium 1.8 nm.

Thermal Characterization. Bulk PVA has a glass transition at $T \simeq 70$ °C and a melting transition at $T_m \simeq 225$ °C. For fully intercalated PVA hybrids [i.e., all the polymer is intercalated in MMT galleries] DSC does not detect any traces of thermal transitions be-
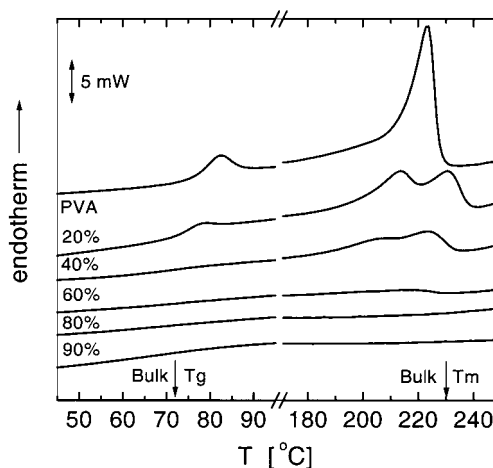
Figure 3. Differential scanning calorimetry of PVA/MMT nanocomposites with varying ϕ_{MMT} (20 °C/min, second heating). For clarity, a featureless region is omitted between 95 and 175 °C.

tween 35 and 250 °C (Figure 3, hybrids with $\phi_{MMT} > 60$ wt %). For these "neatly intercalated" nanocomposites, both the T_g and T_m are too weak and/or too broad to measure, or they are suppressed due to the polymer confinement. Although the physical origins of this behavior are still under debate,[16,17] this absence of thermal events is in agreement with the general behavior of polymers intercalated in clays and synthetic silicates. In a plethora [nylon-6,[2] PEO,[9,10] PMPS,[16] PS,[17] PCL,[18] and PMMA[19] intercalated in naturally occurring silicates (MMT) and in synthetic layered aluminosilicates (FH)] of systems studied, there exist no detectable thermal transitions for the intercalated polymers, over a wide temperature range below the T_g and above the T_m. Despite the use of methods with an increasing resolution and sensitivity (such as DSC, thermally stimulated current, positron annihilation, NMR, and so on), no transitions can be detected in neatly intercalated systems. For example, TSC, DSC, and NMR studies[9,10] of an intercalated poly(ethylene oxide) (PEO, $M_w =$ 100 000)/MMT hybrid (20 wt % polymer) indicated the absence of any thermal transitions between -100 and 120 °C that could correspond to the vitrification or the melting of PEO ($T_g \cong -55$ °C and $T_m \cong 65$ °C). On a local scale, intercalated polymers exhibit simultaneously fast and slow modes of segmental relaxations for a wide range of temperatures,[10,16,17] but again with a marked suppression (or even absence) of cooperative dynamics typically associated with the glass transition.

A systematic study of the DSC traces with ϕ_{MMT} (Figure 3) shows that the T_g and T_m signals weaken gradually and disappear for ϕ_{MMT} above 60 wt %. This suggests that in these systems ($\phi_{MMT} \geq 60$ wt %) all the polymer is affected by the inorganic layers, and there seems to be no bulklike PVA present (at least not enough to manifest itself through thermal transitions). For higher polymer concentrations (e.g., 20 wt % MMT) there appear two distinct and overlapping melting peaks: one around the bulk T_m and another one at higher melting temperature.
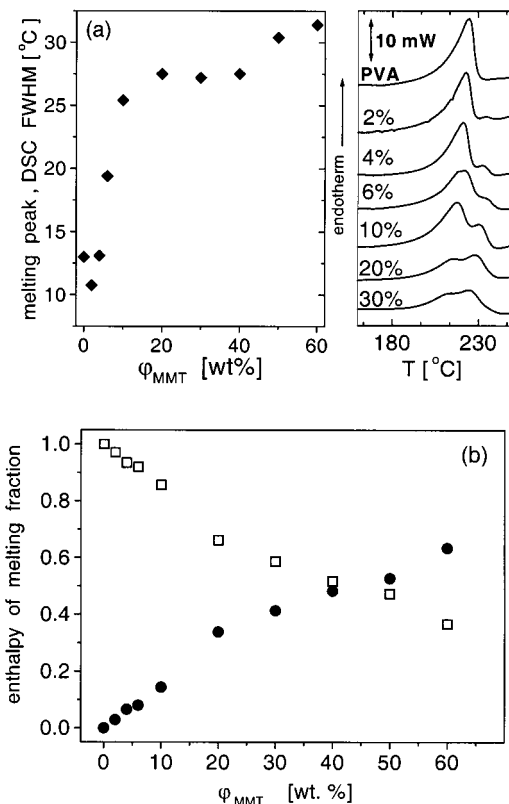
(14) Vaia R. A.; Giannelis, E. P. *Macromolecules* **1997**, *30*, 7990, 8000.
(15) Balazs, A. C.; Singh, C.; Zhulina, E. *Macromolecules* **1998**, *31*, 8370.

(16) Anastasiadis, S. H.; Karatasos, K.; Vlachos, G.; Giannelis, E. P.; Manias, E. *Phys. Rev. Lett.* **2000**, *84*, 915.
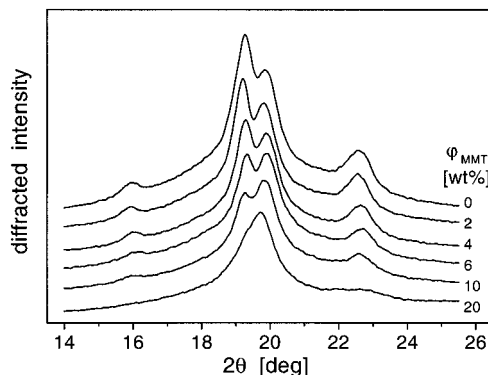(17) Zax, D. B.; Yang, D. K.; Santos, R. A.; Hegemann, H.; Giannelis, E. P.; Manias, E. *J. Chem. Phys.* **2000**, *112*, 2945.

Figure 4. DSC of the melting region for the low MMT content nanocomposites (20 °C/min): (a) fwhm of the combined melting endotherms and corresponding DSC traces around T_m; (b) the fractional heat of fusion owing to the MMT-induced crystal phase (circles, $T_m \simeq 235$ °C) and bulklike crystal phase (squares, $T_m \simeq 225$ °C), as determined from the DSC peak fittings.

Polymer Crystallinity. The PVA melting was studied by performing DSC on several high PVA concentration nanocomposites [$2 \le \phi_{MMT} \le 30$ wt %, Figure 4a]. Compared to the neat PVA, in the nanocomposites appears also a new higher-T_m crystal phase. [Through XRD we will show that this is actually a new phase, rather than a higher T_m morphology with bulk PVA crystal structure.] This dual DSC melting trace is reminiscent of DSC endotherms belonging to a PVA system studied by Tanigami et al.[20] In their system, Tanigami et al. controlled the PVA stereoregularity by using blends of a syndiotactic-rich and an atactic poly-(vinyl alcohol). What was observed was a crystalline-phase-separated system that exhibited a dual melting point. That dual melting point arose from two crystal phases: one formed primarily by syndiotactic sequences and the other primarily by atactic sequences. The two types of crystals have melting points that differ by about 15–22 °C (T_m at 228 and 250 °C). This T_m difference is comparable to the one measured for our PVA/MMT nanocomposites, as shown in Figure 4. The width at half-maximum (fwhm), for the combined DSC melting peak, was used[20] as an indicator of how the two crystal phases were present in the PVA blend. To calculate

(18) Messersmith, P. B.; Giannelis, E. P. *Chem. Mater.* **1993**, *5*, 1064.
(19) Bandyopadhyay, S.; Giannelis, E. P. *Polym. Mater. Sci. Eng.* **2000**, *82*, 208.
(20) Tanigami, T.; Hanatani, H.; Yamaura, K.; Matsuzawa, S. *Eur. Polym. J.* **1999**, *35*, 1165.

Figure 5. XRD of the PVA crystalline peaks as a function of the ϕ_{MMT} in the nanocomposite. The difference between the dual reflection ($10\bar{1}$ and 101) for the bulk PVA ($\phi_{MMT} = 0$) and the reflection for $\phi_{MMT} = 20$ wt % suggests that MMT promotes a new crystal phase with a different crystalline structure (see also Figure 4).

fwhm, the peak value of the DSC trace is located. The full width of the melting peak is then evaluated at a distance halfway between the peak value and the DSC trace baseline. In Tanigami's work, the melting peak fwhm increased to 25–35 °C when the atactic-rich and the syndiotactic-rich phases coexisted, whereas it remained approximately 10 °C when either of the two crystal phases was in excess. [Obviously, when taking the fwhm for the combined DSC melting peak, one is not sensitive to small (smaller than half-maximum) melting peaks.] The fwhm for our nanocomposite combined/dual melting peaks is plotted in Figure 4a as a function of the silicate loading (ϕ_{MMT}). The full width increases sharply from about 13 °C to above 25 °C as the silicate composition crosses the percolation threshold ($\phi_{MMT} \cong 4$ wt %). This suggests that we have substantial volumes of bulklike and of MMT-induced crystal phases coexisting for $\phi_{MMT} > 5$ wt %.

To quantify the relative volumes of the two crystal phases present, we used the standard fitting method[21] and Gaussian functions to estimate the melting enthalpies (heat of fusion, ΔH) for each of the two melting peaks in the DSC trace. The fraction of the two melting enthalpies (Figure 4b) will reflect the relative amount of the respective crystalline phases in the polymer matrix. The new crystal form—which appears when MMT fillers are added to the PVA—seems to grow linearly with the MMT concentration and at the expense of the bulklike PVA crystal phase (Figure 4b). This clearly suggests the high-T_m phase is induced by the presence of the silicate layers. The shape of the melting peak and the relative peak areas remain the same in subsequent DSC scans, after cooling from the melt state (exotherms not shown), thus indicating that this dual crystalline melting is not an artifact of the solution casting or the thermal history but is indeed induced by the presence of the silicate.

Wide angle XRD provides evidence that we actually have a new crystal phase in the nanocomposite. Namely, in the 2θ region between 14.0° and 25.5° (Figure 5) PVA has its 100, $10\bar{1}$, 101, and 200 crystalline reflections (corresponding to $2\theta = 16.0°$, 19.4°, 20.1°, and 22.7°, respectively). In the same region MMT also has its 101

(21) Perkin-Elmer DSC7 Manual, 1994.

reflection at 19.7°. We have annealed our samples at 245 °C for 35 min prior to scanning in order to allow for higher quality PVA crystals. Samples showed some degradation by becoming brown in color, and the overall crystallinity did decrease somewhat; however, the DSC of the annealed samples remains the same qualitatively (dual melting peak) and quantitatively (heat of fusion). The XRD scans in Figure 5 suggest that as silicate content increases from $\phi_{MMT} = 0$ to 20 wt %, the 101 and 10$\bar{1}$ peaks *concurrently* become lower in intensity and are replaced by what appears to be a single peak centered at $\theta \simeq 19.5°$. This is consistent with the DSC measured high-T_m crystal phase that appears at these compositions and with its gradual enhancement at the expense of the bulklike crystal. Unfortunately, a quantitative comparison between the DSC and the XRD is not possible, as the existence of five overlapping diffracted reflections does not allow for the unambiguous fitting of the XRD peaks.

In summary, the analysis of the PVA crystalline XRD and DSC data shows that at low silicate loadings (below 60 wt %) there appears a new crystalline phase, which is induced by the presence of MMT. This phase grows linearly with ϕ_{MMT} at the expense of the bulk PVA crystal phase. For $\phi_{MMT} > 60$ wt %, PVA is primarily intercalated, and no melting endotherms are found for the confined polymer.

Mechanical Properties. Exfoliated polymer/silicate systems have been found to exhibit mechanical, thermal, and solubility properties, as well as water vapor transmission rates, that are superior to conventionally filled systems.[2,6] Furthermore, due to their nanoscale dispersion of filler, they retain optical clarity.[22] In our PVA/MMT hybrids, and especially at the application-relevant low ϕ_{MMT} [below 10 wt %], TEM and XRD reveal a coexistence of intercalated and exfoliated silicate layers. For these systems we will briefly describe some of their materials properties.

Tensile tests were performed on PVA nanocomposite films with silicate loadings of 0, 2, 4, 6, and 10 wt %. Because completely dry PVA films are quite brittle, tests were performed at a nominal relative humidity of 50%, according to the usual testing procedure for PVA.[23] Prior to testing, films were equilibrated in a humidity chamber at 90% relative humidity. Yielding was not found for any of the samples. All samples had an initial period of elastic deformation followed by a nearly monotonically increasing stress during plastic deformation, until failure.

Figure 6 shows the Young's modulus, the stress-at-break and strain-at-break, and the measured fracture toughness, all as a function of silicate loading. For comparison, the Young's moduli are normalized by the measured bulk PVA value (68.5 MPa). At $\phi_{MMT} = 4$ wt %, the nanocomposite is characterized by a modulus about 300% larger than the one of the respective bulk PVA. In most conventionally filled polymer systems, the modulus increases linearly with the filler volume fraction; whereas, for these nanoparticles much lower filler
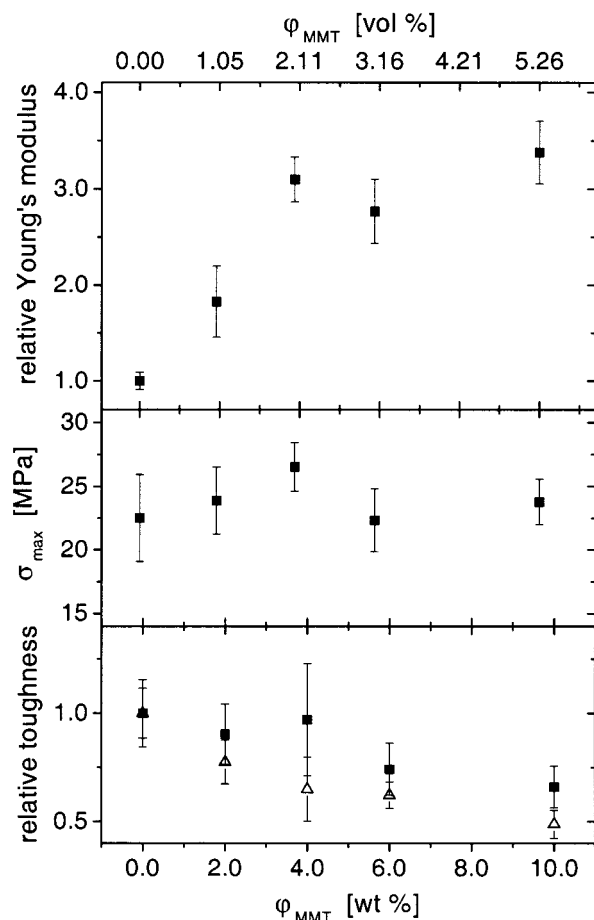
Figure 6. Tensile testing results as a function of MMT weight and volume content. From top to bottom: the Young's modulus normalized by the bulk value (68.5 MPa); the maximum stress at break; the toughness (squares) and strain at break (triangles) of the hybrids normalized by the bulk values (45.8 MPa and 330%, respectively).

concentrations increase the modulus sharply and to a much larger extent.[1] Accordingly, in our PVA/MMT systems the dependence of modulus on ϕ_{MMT} is very strong at very low content and tends to level off after $\phi_{MMT} = 4$ wt %, at about 3.5–4 times the value for bulk PVA. This behavior has been reported before for poly(dimethylsiloxane)/MMT exfoliated hybrids (Figure 2 of ref 24).[25] The dramatic enhancement of the Young's modulus for such extremely low MMT filler concentrations cannot be attributed simply to the introduction of the higher modulus inorganic filler layers. A recent theoretical approach is assuming a layer of affected polymer on the filler surface, with a much higher Young's modulus than the bulk equivalent polymer.[24] This affected polymer can be thought of as the region of the polymer matrix that is physisorbed on the silicate surfaces, and is thus stiffened through its affinity for and adhesion to the filler surfaces.[24] Obviously, for such high aspect ratio fillers as our MMT layers, the surface area exposed to polymer is huge (for MMT is typically 700–800 m²/g), and the dramatic increases in the modulus with very low ϕ_{MMT} are not surprising. Furthermore, beyond the percolation limit ($\phi_{MMT} \geq 4$ wt %)

(22) Wang, Z.; Pinnavaia, T. J. *Polym. Mater. Sci. Eng.* **2000**, *82*, 274. (b) Brown, J. M.; Curliss, D. B.; Vaia, R. A. *Polym. Mater. Sci. Eng.* **2000**, *82*, 278.

(23) Sundararajan, P. R. In *Polymer Data Handbook;* Mark, J. E., Ed.; Oxford University Press: New York, 1999; p 894.

(24) Shia, D.; Hui, C. Y.; Burnside, S. D.; Giannelis, E. P. *Polym. Compos.* **1998**, *19*, 608.

(25) Burnside, S. D.; Giannelis, E. P. *Chem. Mater.* **1995**, *7*, 1597.
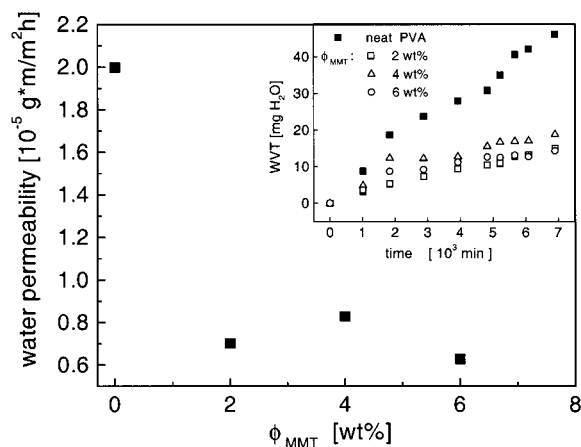
Figure 7. Water vapor permeability for the neat PVA and several PVA/MMT nanocomposites. The inset shows the water vapor transmission raw data collected for each composition, which were used to calculate the water permeabilities.

the additional exfoliated layers are introduced in polymer regions that are already affected by other MMT layers, and thus it is expected that the enhancement of Young's modulus will be much less dramatic.

The stress at break (σ_{max}) is also plotted versus the silicate content in Figure 6. The data show that σ_{max} is relatively insensitive to the filler concentration. Finally, the toughness is also plotted in the same graph, again normalized by the bulk PVA value (45.8 MPa) for comparison; the toughness was calculated from the integrated area under the Instron stress/strain curve. There is a very moderate decrease of the toughness (3% at ϕ_{MMT} = 4 wt % and 22% at ϕ_{MMT} = 6 wt %) with ϕ_{MMT}, which is caused by a comparable decrease of the strain-at-break.

Other Materials Properties. With the dispersion of these ultrathin inorganic layers throughout the polymer matrix, the barrier properties of the nanocomposites are expected to be strongly enhanced compared to the respective polymer. The water vapor transmission rates were measured for the pure polymer and several of its low ϕ_{MMT} nanocomposites and are plotted in Figure 7. In the same figure, the resulting water permeabilities[13] are plotted as well. WVT and permeabilities were measured following ASTM E96, for PVA and PVA/MMT nanocomposite films of the same thickness ((8.98 ± 0.33) $\times 10^{-3}$ cm). The permeabilities decrease to about 40% of the pure WVT values for silicate loadings of only 4−6 wt %. We believe that this enhancement in the water permeability originates from the increased path tortuosity of the penetrant molecules—forced around the inorganic layers—as well as the enhanced modulus of the polymer matrix in the nanocomposites.

Because of the nanoscale dispersion of the silicates in the PVA matrix, optical clarity remains high at silicate contents which yield primarily exfoliated composites. This allows its potential use in paper coatings, one of the most common uses for pure PVA. Figure 8a shows the UV/vis transmission spectra of pure PVA and PVA/MMT hybrids with 4 and 10 wt % MMT. These films have thicknesses of 0.17, 0.18, and 0.15 mm, respectively. The spectra show that the visible region (400−700 nm) is not affected at all by the presence of the silicate and retains the high transparency of the PVA. For the ultraviolet wavelengths, there is strong
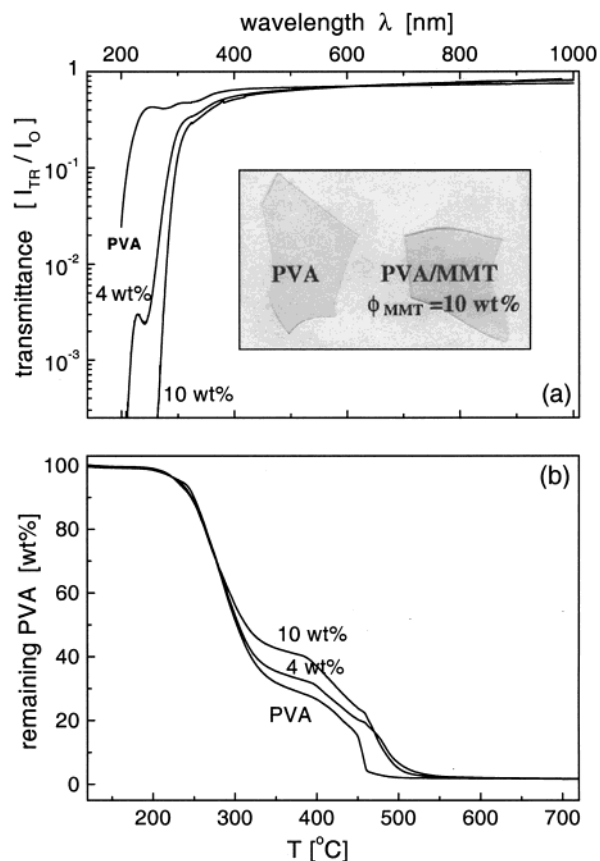
Figure 8. (a) UV−vis transmittance spectra of PVA and PVA/MMT nanocomposites containing 4 and 10 wt % MMT. (b) Polymer weight loss from TGA scans in air, for PVA and two nanocomposites containing 4 and 10 wt % Na$^+$ MMT.

scattering and/or absorption, resulting in very low transmission of the UV light. This is not surprising as the typical MMT lateral sizes are 50−1000 nm.

In addition to having a higher melting point, thermal degradation properties of PVA/MMT nanocomposites also show improvement. A comparative thermal gravimetric analysis (TGA) of pure PVA and two nanocomposites with 4 and 10 wt % MMT (10 °C/min in air) is shown in Figure 8b. The weight loss due to the decomposition of PVA is nearly the same until the temperature of about 275 °C. After this point, the silicate inhibits the PVA weight loss, which reaches a maximum lag of about 75 °C. Unlike most other polymer/MMT nanocomposite systems,[19] this PVA/MMT suffers nearly the same weight loss as the bulk for its initial 50%, possibly due to the fact that PVA can supply oxygen from within to initiate its decomposition.

Conclusions

We have investigated the structure and properties of PVA/MMT nanocomposites formed by water casting, a solution intercalation method. From TEM and XRD studies, over the full range of silicate loadings, we find that there is a coexistence of exfoliated and intercalated silicate layers. The system becomes mostly intercalated as silicate loading increases beyond $\phi_{MMT} \geq 60$ wt %. The exfoliation of layers is attributed to the water casting method used, since the water suspended layers become kinetically trapped by the polymer and cannot reaggregate. DSC studies find a suppression of the

Poly(vinyl alcohol)/Na⁺ Nanocomposites

Chem. Mater., Vol. 12, No. 10, 2000 **2949**

thermal transitions (T_g and T_m) for the purely intercalated systems. However, for the mostly exfoliated, low MMT loading nanocomposites, DSC unveils a new melting transition with higher T_m than the neat PVA. X-ray diffraction of the polymer crystals suggests that this is a new, silicate-induced PVA crystal phase promoted by the existence of the montmorillonite layers at the expense of the bulklike PVA crystalline phase.

Some basic materials characterization was also performed, for the low ($\phi_{MMT} \leq 10$ wt %) MMT loadings. For these MMT concentrations the inorganic layers are well dispersed throughout the PVA matrix; i.e., the nanocomposites formed are mostly-exfoliated hybrids. The mechanical/tensile properties of these nanocomposites were studied for low silicate loadings, and Young's modulus was found to increase by 300% for 5 wt % silicate, with only a 20% decrease in toughness, and no sacrifice of the stress at break compared to the case of neat PVA. In addition, for these low loadings, thermal stability from TGA measurements was shown to be slightly enhanced, and high optical clarity was retained. Additional properties at low silicate loadings, detailed AFM studies of the PVA crystal morphology, and NMR investigations of the PVA segmental dynamics in intercalated structures are currently underway.

CM000506G